ELSEVIER

Journal of Nuclear Materials 258–263 (1998) 124–129

journal of nuclear materials

# Hydrogen inventory and embrittlement in low activation steels

P. Jung [1]

*Institut für Festkörperforschung, Forschungszentrum Jülich, Association EURATOM-FZJ, D-52425 Jülich, Germany*

**Abstract**

Results on hydrogen permeation and diffusion in virgin and preirradiated iron and martensitic MANET II are compared to literature data on iron and other ferritic/martensitic steels. Both permeability and diffusivity decrease with increasing alloying content. While preirradiation to $1.5 \cdot 10^{-3}$ dpa has negligible effect on permeation and diffusion, simultaneous irradiation enhances permeability in Fe and MANET II below ≈300°C. Diffusivity shows a strong pressure dependence and deviation from Arrhenius-type temperature dependence. Diffusion of implanted hydrogen shows a behaviour different from that derived from gas permeation. The hydrogen inventory in a fusion reactor blanket is roughly estimated and compared to the critical concentration for hydrogen embrittlement. Hardness of hydrogen implanted MANET II and F82H shows no pecularities compared to helium implantation and only slightly differs from irradiation without implantation. Tensile tests on F82H at 30°C and 200°C after implantation to hydrogen concentration above ≈10 wtppm show large variation, possibly due to formation of microcracks, while measurements at 350°C show no effect of implantation. 

## 1. Introduction

Low activation martensitic stainless steels are candidate materials for first wall and blanket structures of future fusion reactors, mainly due to their stability against swelling and helium embrittlement. On the other hand, hydrogen uptake and permeation and, as possible consequences, mechanical degradation and contamination by tritium are major concerns.

## 2. Permeation

Basic material properties which determine hydrogen inventory are permeability $P$, diffusivity $D$ and solubility $S$, which are interrelated by

$$P = SD. \quad (1)$$

Fig. 1 reviews recent results on permeability measurements in 7–12% Cr martensitic steels. There is a clear tendency of permeability to decrease with increasing alloying content, mainly due to an increase of activation energy, cf. Ref. [1].

The solid symbols in Fig. 1 indicate specimens which were predamaged by proton irradiation to about $1.5 \cdot 10^{-3}$ dpa, giving no perceivable effect in the steel, while the small difference for iron is probably an isotope effect. On the other hand simultaneous irradiation by a 0.5 μA proton beam yields significantly enhanced permeability (Fig. 2). The additional permeation flux per beam flux also depends on temperature and is for iron by about one order of magnitude higher than for MANET [5]. For austenitic steels enhancement of permeability by more than one order of magnitude has been reported under reactor irradiation [6,7]. This larger relative effect in austenitics is probably due to their lower base permeability (Fig. 1). A comparison of the few available results on irradiation effects indicates that the main reason for the enhanced permeability is probably ionisation of the gas on the upstream side [5].

## 3. Diffusion

Diffusivity is derived from pressure transients of permeation measurements. A compilation of apparent diffusivity data of iron and martensitic stainless steels is

[1] Tel.: +49-2461 614 036; fax: +49-2461 612 410; e-mail: p.jung@fz-juelich.de.

0022-3115/98/$19.00 
PII: S0022-3115(98)00326-2

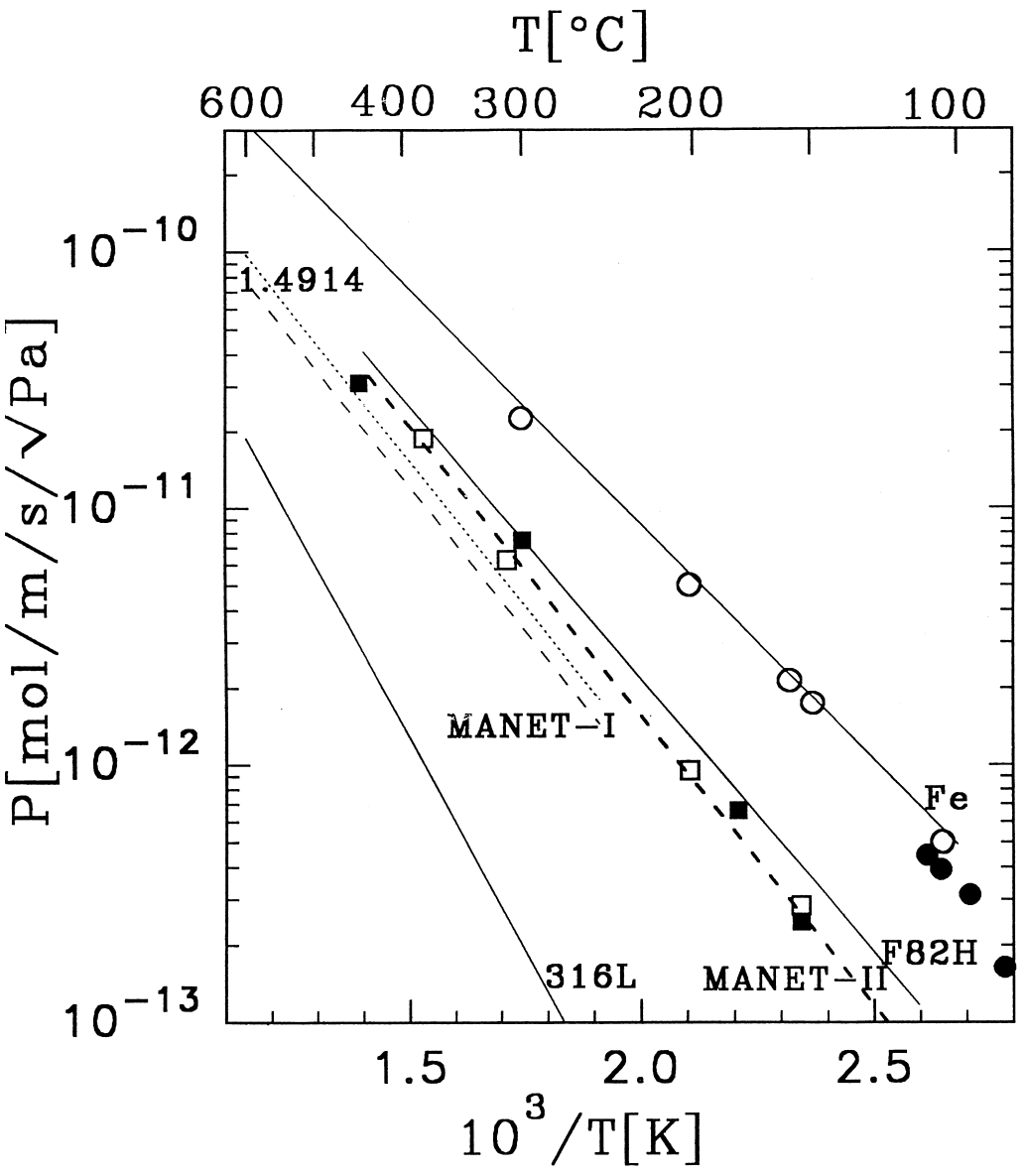


Fig. 1. Temperature dependence of permeabilities of $H_2$ (○) and $D_2$ (●) in Fe and of $H_2$ (□, ■) in MANET II (thickness 210 μm). Filled symbols indicate specimens preirradiated by 12.3 MeV protons to about $1.5 \cdot 10^{-3}$ dpa. Lines give literature data for iron (averaged) [2], for F82H and MANET II [3], and for DIN1. 4914, MANET I and austenitic 316L [4] as indicated.

given in Fig. 3. The tendency of reduction by alloying is stronger than in the case of permeability in Fig. 1. Furthermore at temperatures below 300°C strong deviations from the Arrhenius-type behaviour at high-temperatures are observed in the alloys. This temperature dependence as well as a strong pressure dependence of diffusivity [5] can be quantitatively fitted by a model for trapping of hydrogen by saturable traps, as developed in Refs. [11,12]:

$$D = D_0 \exp(-E_m/RT)/(1 + n_T \exp(E_b/RT)). \quad (2)$$

Parameters derived from these fits ($D_0 = 4.5 \cdot 10^{-8}$ m$^2$/s, $E_m \approx 10$ kJ/mol) are a binding energy $E_b$ of hydrogen to traps of about 64 kJ/mol and a relative trap concentration $n_T \approx 5 \cdot 10^{-7}$ per interstitial site. Calculation of solubility by Eq. (1) gives an almost constant value of $\approx 10^{-3}$ mol $H_2/m^3/\sqrt{Pa}$ below 300°C, i.e. about 0.08 wtppm hydrogen at 1 bar.

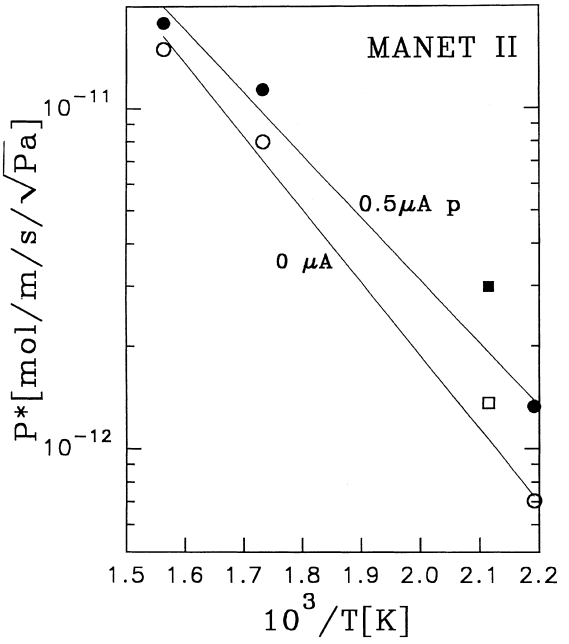


Fig. 2. Temperature dependence of apparent permeabilities of $H_2$ or $D_2$ in 210 μm (○, ●) and 810 μm (□, ■) MANET II specimens. The filled symbols indicate measurements under 0.5 μA proton irradiation.

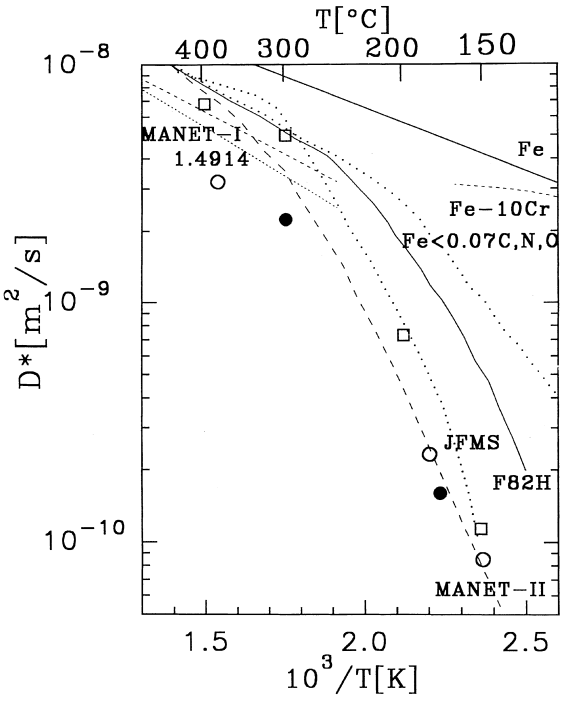


Fig. 3. Temperature dependence of apparent diffusion coefficients in 810 μm ($H_2$, □), and 210 μm ($H_2$, $D_2$, ○) MANET II specimens. The filled circles indicate 210 μm specimens ($H_2$) preirradiated to $1.5 \cdot 10^{-3}$ dpa. Included are literature data for pure iron (–) [8], Fe–10% Cr (- -) [9], Fe with <0.07% C, N, O (···) [24], for Japanese JFMS (···) [10], for F82H (-) and MANET II (- -) [3], and for DIN1.4914 (· ·), MANET I (- -) [4].

In specimens preirradiated to $1.5 \cdot 10^{-3}$ dpa (solid circles in Fig. 3) diffusivity is slightly reduced, corresponding to an increase of the number of traps by about a factor of 2, while the binding energy is virtually unchanged [5]. This binding energy is in the range of values reported for vacancies as well as dislocations and possibly also for grain boundaries; for a compilation compare Ref. [23]. Diffusion constants can also be derived from the release of hydrogen implanted to a certain depth, cf. Refs. [5,13]:

$$D = qx^2/\tau_{1/2}, \tag{3}$$

where $x$ is the diffusion path to the analysed surface, $\tau_{1/2}$ the measured characteristic delay time of the permeation flux after beam on or off, and $q$ includes a numerical factor and also depends on the released fraction of the implanted atoms. The yet limited results [5] give $\tau_{1/2}$ values which are almost independent of $x$, probably indicating that the total diffusion time is dominated by trapping processes in the implantation region [5].

## 4. Hydrogen inventory

Sources of hydrogen for first wall and blanket materials can be subdivided on the one hand into hydrogen production by transmutation reactions, e.g. (n, p) in the bulk of the materials (internal source), and on the other hand into hydrogen entering the materials through the surfaces (external sources).

### 4.1. External sources

The main external hydrogen sources for structures cooled by water or gas are [14]:

1. aqueous corrosion,
2. radiolysis of cooling water,
3. hydrogen added to water as a corrosion inhibitor and
4. hydrogen added to cooling or purging helium gas.

Hydrogen implantation from the plasma into the first wall structure can be disregarded due to shielding by low $Z$ materials. The first two processes are supposed to produce comparatively small amounts of hydrogen, with one possible point of concern being the production of nascent $H^+$ with its much higher reactivity. On the other hand it is believed that recombination is ubiquitous and prevents $H^+$ to extensively interact with the materials surfaces. The effect of the last two sources depends on hydrogen solubility in the materials. Table 1 lists hydrogen concentrations in the bulk resulting from typical hydrogen additions to coolants, using below 300°C the

Table 1
Hydrogen concentrations in low activation martensitic steels from hydrogen added to coolants

| Coolant | $c_{H_2}$ in coolant [wtppm] | $p_{H_2}$ [Pa] | $T$ [°C] | $c_H$ in LAM [wtppm] |
|---|---|---|---|---|
| $H_2O$ | 1.3 [a] | 180 | 300 | 0.04 |
| He | $2.5 \cdot 10^4$ | $10^5$ | 250 | 0.08 |
| He | $2.5 \cdot 10^4$ | $10^5$ | 550 | 0.6 |

[a] as proposed for boiling water reactors, see Ref. [15].

above value of $10^{-3}$ mol $H_2/m^3$ $\sqrt{Pa}$. All resulting values are well below the critical concentration for hydrogen embrittlement which amounts to $c_H^* \approx 10$ wtppm at room temperature in 9–12% Cr martensitic steels as shown by a recent compilation of experimental data [16].

### 4.2. Inventory from transmutation reactions

A hydrogen generation rate by transmutation reactions $G_0$ of about $6 \cdot 10^{-7}$ wtppm H/s is estimated in the first wall for a wall loading of 2 MW/m$^2$. In a piece of material with impermeable surfaces, e.g. due to barriers, this would cause the hydrogen concentration to reach $c_H^*$ ($\approx 10$ wtppm) within about half a year. On the other hand if a compact blanket sheet of 0.5 m thickness is assumed, with one side permeable, $c_H^*$ is reached only for operation temperatures below ≈230°C after an operation time of about 3 years [16]. It depends on the temperature dependence of $c_H^*$ and the detailed blanket design whether this crude estimate is on the optimistic or pessimistic side.

## 5. Mechanical properties

The compilation in Ref. [16] showed that only two studies have so far attempted to investigate the effect of irradiation on critical concentration $c_H^*$, most probably indicating a reduction of $c_H^*$ by irradiation [17,18]. In an attempt to broaden the experimental database, experiments were performed on specimens which were implanted by energetic protons, the energy of which was moderated by a degrader wheel with aluminium foils of varying thicknesses, to obtain a homogeneous distribution [19]. During implantation the specimens were contacted to a copper heat sink with a solder of ≈70°C melting temperature. For an estimated irradiation temperature of 50°C this corresponds according to Eq. (2) to a maximum effective diffusion coefficient of about $D^* \leqslant 10^{-13}$ m$^2$/s. For slab geometry with permeable surfaces the evolution of concentration in the centre is given by, cf. Ref. [16]:

$$c_{max}(t) = Gd^2(1 - e^{-t/\tau})/8D \quad (4)$$

with $\tau \approx 0.1d^2/D$ being the characteristic time of concentration build up or decay during beam on and off periods, respectively. For a homogeneously implanted specimen of thickness $d \approx 400$ μm and a generation rate $G \approx 1.5 \cdot 10^{-4}$ wtppm/s this gives an asymptotic value $c_{max} \approx 30$ wtppm reached after a characteristic time $\tau \approx$ 44 h. For the hardness measurements the 400 μm specimens were homogeneously implanted only to a depth of ≈110 μm. In this case $c_{max}$ and $\tau$ are in the order of 2 wtppm and 3 h, respectively. From this rough estimate it must be concluded that only in the tensile but not in the hardness specimens the critical hydrogen concentration was reached during implantation.

### 5.1. Hardness

Figs. 4 and 5 show microhardness data $H_p$ of MANET II and F82H specimens implanted with hydrogen, helium or both to various concentrations. In Fig. 6 interpolated changes of hardness by irradiation or hydrogen implantation as derived from these figures are given as a function of displacement dose. For calculation of the displacement doses, factors of 9 and 70

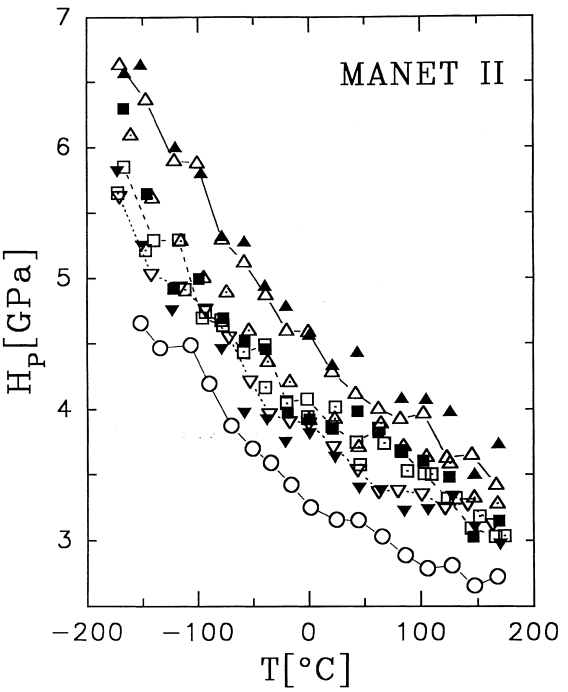


Fig. 4. Microhardness $H_p$ versus measuring temperature of MANET II specimens unirradiated (○, -) and implanted with hydrogen to nominally 500 (▽, ···), 2500 (□,- -) and 12500 (△, -) atppm (corresponding to 9, 43 and 215 wtppm, respectively), with helium to 500 (⊡) and 2500 (▽) atppm (corresponding to 34 and 172 wtppm, respectively), and with both H and He to 500 + 100 (▼), 2500 + 500 (■), and 12500 + 2500 (▲) atppm.

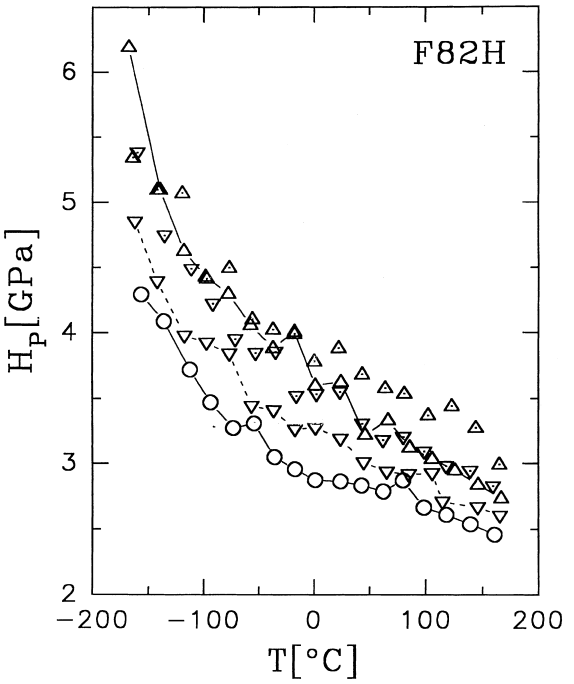


Fig. 5. Microhardness $H_p$ versus measuring temperature of F82H specimens unirradiated (○, -) and implanted with hydrogen to nominally 1500 (▽, –), and 5000 (△, - -) atppm (corresponding to 26 and 86 wtppm, respectively), and with helium to 300 (△) and 1000 (▽) atppm (corresponding to 21 and 69 wtppm), respectively.

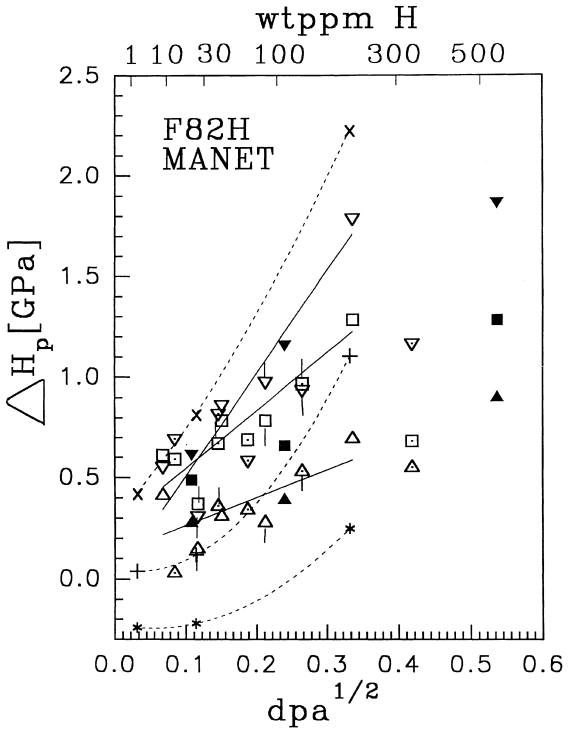


Fig. 6. Change of microhardness of irradiated MANET II (*, +, x) and of MANET II and F82H (F82H indicated by pins) specimens implanted with hydrogen (empty) and helium (dotted symbols) and H + He (filled) as a function displacement dose at temperatures of −150° (×, ▽), 0° (+, □) and +170°C (*, △). The dashed lines give eye-fits through the data of irradiated MANET II without implantation for the three temperatures, and the solid lines through the data of implanted MANET II and F82H. The upper scale gives the calculated nominal hydrogen concentrations in the hydrogen implanted specimens.

displacements per implanted hydrogen (maximum energy 6.5 MeV) or helium ion (maximum energy 26.3 MeV) were used, respectively [20]. Within the scatter of data there is no difference in hardness for specimens implanted with hydrogen, helium or both, when compared on the basis of displacement damage. On the other hand the data after irradiation of MANET without implantation, cf. Ref. [21], are slightly different, showing somewhat higher hardness at the lower temperatures and lower hardness at the higher temperatures, with even some softening at low doses. This indicates that the major part of hardening is due to displacement defects, with the implanted atoms giving possibly some contribution at the higher temperatures. This contribution is also present after hydrogen implantation, although it is not clear whether the nominal amount of hydrogen is actually retained in the specimens.

### 5.2. Tensile tests

Miniaturized specimens of 400 μm thickness, 1.5 mm width and ≈7 mm gauge length were homogeneously implanted with protons of a maximum energy of 12.5 MeV, corresponding to ≈14 displacements per implanted H atom. They were tensile tested in vacuum at 30°C, 200°C and 350°C at strain rates from $7 \cdot 10^{-5}$ to $9 \cdot 10^{-4}$/s. At implanted concentrations up to about 7 wtppm, yield stress and ultimate tensile strength increased at room temperature while at 200°C both stresses slightly decreased (Fig. 7). Uniform and total elongations slightly decreased at *RT* and 200°C. Practically no effect of hydrogen implantation on strengths and elongations was observed at 350°C, probably indicating complete hydrogen release below this temperature. The slight increase in strength at *RT* is in good agreement with results on MANET at 80°C [22]. At higher concentrations strengths and elongations show large specimen to specimen variations at *RT* and 200°C. This is tentatively ascribed to the formation of microcracks when the critical concentration for hydrogen embrittlement is exceeded. Further tensile and microscopial investigations in this concentration regime are necessary.

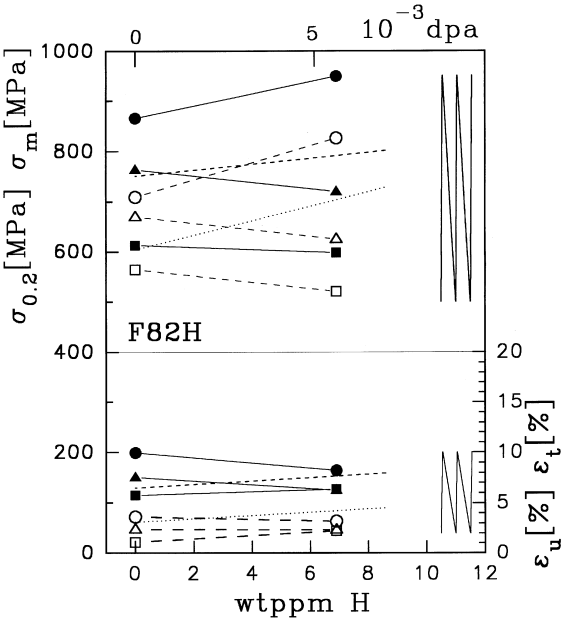


Fig. 7. Yield strength $\sigma_{0.2}$ (empty symbols), engineering tensile strength $\sigma_m$ (filled), uniform elongation $\epsilon_u$ (empty) and total elongation $\epsilon_t$ (filled) of 400 μm F82H specimens homogeneously implanted at $\leqslant$70°C with hydrogen, measured at 30° (○), 200° (△) and 350°C (□), respectively. The dotted and short-dashed lines give $\sigma_{0.2}$ and $\epsilon_u$, respectively $\sigma_m$ and $\epsilon_t$ of hydrogen implanted MANET measured at 80°C [22]. Above ≈10 wtppm the data show very large scatter.

## 6. Summary and conclusions

Permeability of hydrogen in martensitic stainless steels

- tends to decrease with increasing alloying content,
- shows negligible effect of preirradiation at low doses, and
- is enhanced under simultaneous irradiation.

Diffusivity

- also tends to decrease with increasing alloying content,
- shows pressure dependence and deviation from Arrhenius-type temperature dependence below ≈300°C.
- Diffusivity of implanted hydrogen shows a much lower temperature dependence.

Solubility

- becomes almost independent of temperature below 300°C.

Hydrogen production by nuclear reactions

- may pose problems if no provision is made for draining.

Hardness of martensitic steels

- is enhanced mainly by displacive irradiation with a lesser contribution from implantation, which slightly increases with measuring temperature.

Strength and ductility of hydrogen implanted martensitic steels

- are slightly increasing, respectively, decreasing below 7 wtppm at room temperature,
- show large fluctuations above ≈10 wtppm at *RT* and 200°C and are virtually unchanged at 350°C.

## Acknowledgements

Contributions of J. Chen and H. Klein to mechanical testing are gratefully acknowledged.

## References

[1] P. Jung, J. Nucl. Mater. 238 (1996) 189.
[2] O.D. Gonzales, Trans. Met. Soc. AIME 246 (1969) 607.
[3] E. Serra, A. Perujo, G. Benamati, J. Nucl. Mater. 245 (1997) 108.
[4] K.S. Forcey, D.K. Ross, J.C.B. Simpson, J. Nucl. Mater. 160 (1988) 117.
[5] F. Wedig, P. Jung, J. Nucl. Mater. 245 (1997) 138.
[6] B.G. Polosukhin, E.P. Baskakov, E.M. Sulimov, A.P. Zyrianov, Y.S. Shestakov, G.M. Kalinin, Y.S. Strebkov, A.G. Dobrynskih, J. Nucl. Mater. 191–194 (1992) 219.
[7] B.G. Polosukhin, E.M. Sulimov, A.P. Zyrianov, A.V. Kozlov, J. Nucl. Mater. 233–237 (1996) 1174.
[8] Compilation by J.Völkl and G. Alefeld in Hydrogen in Metals I, in: G.Alefeld, J.Völkl (Eds.), Springer, Berlin, 1978 p. 321.
[9] E.W. Johnson, M.L. Hill, Trans. Met. Soc. AIME 218 (1960) 1104.
[10] E. Hashimoto, T. Kino, J. Nucl. Mater. 133&134 (1985) 289.
[11] A. McNabb, P.K. Foster, Trans. Met. Soc. AIME 227 (1963) 619.
[12] H.H. Johnson, Metall. Trans. A 19 (1988) 2371.
[13] F. Wedig, PhD thesis RWTH Aachen, Report Forschungszentrum Jülich Jül-3334 (1996).
[14] R. Boler, C.B.A. Forty, G.J. Butterworth, Report AEA FUS 164 (1992).
[15] R.L. Jones, C.J. Wood, R.L. Covan, R.A. Head, C.C. Lin, T.L. Wong, Nucl. Engg. Int. 1987, p. 25.
[16] P. Jung, Fusion Technol. 33 (1998) 63.
[17] J. Koutsky, K. Spichal, Int. J. Press. Vess. Piping 24 (1986) 13.
[18] A. Kimura, H. Kayano, M. Narui, J. Nucl. Mater. 179–181 (1991) 737.
[19] P. Jung, V. Sciani, in Diffusion in Metals and Alloys, in: F.J. Kedves, D.L. Beke, Trans. Tech. Publ., 1983, p. 446.
[20] P. Jung, in Landolt-Börnstein, New Series, Group III, Springer, Berlin, vol. 25, 1991 p. 1.
[21] J. Chen, P. Jung, J. Nucl. Mater. 212–215 (1994) 559.
[22] K.K. Bae, K. Ehrlich, A. Möslang, J. Nucl. Mater. 191–194 (1992) 905.
[23] J.P. Hirth, Metall. Trans. A 11A (1980) 861.
[24] H.-J. König, K.W. Lange, Arch. Eisenhüttenwes. 46 (1975) 669.